Supporting information

Microscopic local stiffening in supramolecular hydrogel network expedites stem cell mechanosensing in 3D and bone regeneration

Weihao Yuan, Haixing Wang, Chao Fang, Yongkang Yang, Xingyu Xia, Boguang Yang, Yuan Lin, Gang Li*, Liming Bian**

Mr. W. Yuan, Dr. B. Yang, Prof. L. Bian
Department of Biomedical Engineering, The Chinese University of Hong Kong, Sha Tin, New Territories, Hong Kong, 999077, China
* Corresponding author. Email: lbian@cuhk.edu.hk

Mr. H. Wang, Mr. Y. Yang, Prof. G. Li
Department of Orthopaedic and Traumatology, The Chinese University of Hong Kong, Sha Tin, New Territories, Hong Kong, 999077, China
* Corresponding author. Email: gangli@cuhk.edu.hk

Dr. C. Fang, Mr. X. Xia, Prof. Y. Lin
Department of Mechanical Engineering, The University of Hong Kong, Pok Fo Lam, Hong Kong, 999077, China
* Corresponding author. Email: ylin@hku.hk

Prof. L. Bian
Shenzhen Research Institute, The Chinese University of Hong Kong, Shenzhen, 518172, China

Prof. L. Bian
China Orthopedic Regenerative Medicine Group (CORMed), Hangzhou, Zhejiang, 310058, China

Prof. L. Bian
Centre for Novel Biomaterials, The Chinese University of Hong Kong, Hong Kong, 999077, China

Materials and Methods

Materials

Gelatin type A from porcine skin, 3-(trimethoxysilyl) propyl methacrylate, silver nitrate, deuterium oxide (D_2O), Triton X-100, and bovine serum albumin (BSA) were purchased from Sigma-Aldrich (U.S.A.). Tetraethyl orthosilicate (TEOS), arginine, beta-cyclodextrin (β-CD), acryloyl chloride, triethylamine (TEA), alizarin red and tween-20 were purchased from J&K Scientific (China). All chemicals were used upon received form without any further purification. 4′,6-diamidino-2-phenylindole (DAPI), rhodamine phalloidin, calcein AM, propidium iodide (PI), Dulbecco's phosphate buffered saline (DPBS), fetal bovine serum (FBS), alpha-minimal essential medium (α-MEM), L-glutamine, penicillin/streptomycin (P/S), TRIzol reagent, RIPA buffer, reverseaid first strand cDNA synthesis kit, BCA protein assay kit, calcium quantification kit was purchased from Thermo Fisher (U.S.A.). All antibodies were purchased from Santa Cruz (U.S.A.) unless otherwise specified. Peroxidase substrate DAB kit, and vectorstain ABC kit were purchased from Vector Lab (U.S.A.). Human mesenchymal stem cells (hMSCs) were obtained from Lonza (U.S.A.).

Synthesis of acryloyl beta-cyclodextrin (Ac-β-CD)

Ac-β-CD was synthesized according to previous report[1]. Briefly, 10g of β-CD was dissolved in 150 mL DMF, followed by adding 3.5 mL TEA into the solution. The mixture was cooled down to 0 ℃, and then 2.5 mL acryloyl chloride was added

dropwise into the solution for 1 hour. The reaction was kept stirring for 12 hours under room temperature. The mixture was filtrated to remove precipitated TEA HCl salt, and the obtained clear yellowish solution was concentrated to 20 mL by rotary evaporation system under vacuum condition. The solution was poured into 800 mL acetone to obtain the Ac-β-CD precipitation, and the precipitation was washed with acetone for three times. The substitution degree (S.D.) was determined by ^{1}H nuclear magnetic resonance (^{1}H NMR) on Advanced 400MHz (Bruker, U.S.A.) in DMSO-d6 under room temperature.

Synthesis of silica nanoparticles

The silica nanoparticles with different size were synthesized according to previous report[2]. Briefly, the silica seeds of 30 nm size were synthesized by mixing 9.1 mg L-arginine with 6.9 mL DI water, followed by adding 0.45 mL cyclohexane, and then the mixture was heated to 60 ℃. Once the temperature reached 60 ℃, 0.55 mL of TEOS were added into the vial. The reaction was kept at constant stirring and temperature for 20 h. The silica seeds were collected by centrifugation, and then washed for three times. To regrowth the silica seeds to around 50 nm size, 5 mL as-prepared silica seeds, 2.5 mL cyclohexane, 1.76 mL TEOS were mixed in another flask. The reaction was proceeded for 30 h under constant stirring and temperature of 60 ℃. The regrown silica nanoparticles were collected by centrifugation, and then washed for three times.

Surface modification of silica nanoparticles

The silica nanoparticles were chemically modified with methacryloyl groups according to previous report[3]. Briefly, 0.1 g of silica nanoparticles with different sizes and 2 mL 3-(trimethoxysilyl) propyl methacrylate were added into 50mL toluene. The reaction was kept stirring with nitrogen protection under room temperature for 12 h. The resulting methacryloyl-modified silica nanoparticles were collected by centrifugation, and then washed for three times.

Characterization of silica nanoparticles

Dynamic light scattering (DLS) and zeta potential measurements were conducted on DelsaMax Pro (Beckman Coulter, U.S.A.). Transmission electron microscopy (TEM) was performed on H7700 (Hitachi High Technology, Japan) with an accelerating voltage of 100 kV. Fourier transform infrared spectroscopy (FT-IR) was conducted on Cary 630 (Agilent, U.S.A.).

Fabrication of GHG hydrogels doped with AcNPs

The AcNP-doped hydrogels were fabricated by simply mixing the gelatin, Ac-β-CD, and AcNPs in the phosphate buffer saline (PBS) at 37 ℃. GHG precursor solution with homogeneously dispersed AcNPs (0.4 mg/mL) were formed by the host-guest interactions between the aromatic residues of gelatin (8% (w/v)) and Ac-β-CD (10% (w/v)). The polymerization of GHG hydrogels were conducted by ultraviolet (UV) irradiation for 12 minutes with I2959 (0.05% (w/v)) as the initiator

Rheological and compression measurements

Rheological measurements of the hydrogels were performed on Kinexus Lab plus (Malverm, U.K.). For oscillatory time sweep experiments, the storage modulus (G') and loss modulus (G") were measured under constant strain (0.1%) and frequency (1 Hz). For the oscillatory frequency experiments, the storage modulus (G') and loss modulus (G") were measured under constant strain (0.1%), and the frequency sweep from 10 Hz to 0.1 Hz. For the characterization of shear thinning properties, the hydrogels were sheared by alternating stain of 0.1% and 250% for several cycles. The compression measurements of the hydrogels were performed on Kinexus Lab plus (Malverm, U.K.). The compression rate was set at 0.05 mm/s. The Young's modulus was calculated by the initial linear region of stress-strain curves (strain<10%).

Scanning electron microscopy (SEM) and atomic force microscopy (AFM) experiments

The SEM were conducted on SU8010 (Hitachi High Technology, Japan) with an accelerating voltage of 5 kV. The AFM were performed on NanoWizard II (JPK Instruments, U.S.A.). Pyramid cone AFM tips (Arrow CONT-20, Nano-world, U.S.A.) with spring constant of 0.2N/m were used for all hydrogel samples. The optical sensitivity and spring constant were calibrated by indenting on the glass. To get the young's modulus mapping on the hydrogels, 32 × 32 force mappings were imaged in

10 × 10 um^2 range. 2 μm indentation depths with fast extending and retracting speed were chosen to acquire elastic modules at every point. Modified Hertz models for pyramid cone indenter were chosen. Data was processed by JPK DP software.

Cell culture and osteogenic differentiation induction

Stem cells were expanded to passage 4, and then encapsulated in the hydrogels with the density of 1×10^7/mL. Cells were cultured in the osteogenic medium (α-MEM, 16.67% FBS, 1% glutamine, 1% pen/strep, 1×10^{-2} M β-glycerophosphate disodium, 50 mg mL^{-1} L-Ascorbic Acid 2-phosphate, 1×10^{-7} M dexamethasone), and medium was changed three times per week.

Fluorescent staining and analysis

Live/dead staining was conducted by adding 3μM calcein AM and 3μM propidium iodide working solution to the hydrogels. After incubation for 20 min at 37 ℃, the hydrogels were washed several times with PBS. For the immunofluorescent staining, cells were fixed with 4% paraformaldehyde solution for 1 h at room temperature, followed by 0.1% Triton-X 100 treatment in PBS for 1 h and 3 % BSA blocking in PBS for 2 h. The cytoskeletons were stained with phalloidin-rhodamine, and cell nucleus were stained with DAPI. For YAP staining, the pre-treated samples were incubated with the primary antibody at 4 °C overnight, followed by incubation with the secondary antibody conjugated with FITC for 2h at room temperature. All the fluorescent images

were acquired by C2 plus confocal microscopy (Nikon, Japan), and analyzed by Image J software (NIH). Circularity index of the stem cells encapsulated in hydrogels were calculated based on $F = 4\pi A/P^2$, where A is the cell area and P is the cell perimeter.

Gene expression analysis

For quantitative polymerase chain reaction (qPCR), the samples were harvested and homogenized in 1 mL TRIzol reagent, and total RNA was extracted according to the manufacturer's instructions. The concentration of total RNA was then measured by using a Nanodrop 2000 spectrophotometer. 100 ng of RNA from each hydrogel was reverse transcribed into cDNA by using RevertAid Fist Strand cDNA Synthesis Kit according to manufacturer's protocol. qPCR was performed on StepOnePlus (Thermo, U.S.A.) by using Taqman primers and probes specific for GAPDH (housekeeping gene) and other osteogenic marker genes including alkaline phosphatase, collagen type I, osteocalcin, and runt-related transcription factor 2. The sequence of primers and probes are listed in Table S2. The relative gene expression was calculated by using the $\Delta\Delta C_T$ method. For western blotting, total protein was extracted by using RIPA lysis and extraction buffer and 523 halt phosphatase inhibitor cocktails according to the manufacturer's instructions. The western blotting was performed on mini protein electrophoresis system (Bio-Rad, U.S.A.). After electrophoresis separation, the samples were transferred to a 0.45-mm PVDF membrane (Millipore, U.S.A.). The PVDF membranes were blocked with 5% fat-free milk powder solution for 2 h at room temperature and then incubated with vinculin and p-FAK primary antibodies at 4°C

overnight with gentle rocking. Horseradish peroxidase-coupled secondary antibodies were then applied for 2h at room temperature with gentle rocking. Then, the enhanced chemiluminescence (ECL) substrates (Millipore, U.S.A.) were added on the membranes. The chemiluminescence images were acquired by ChemiDoc (Bio-Rad, U.S.A.) and analyzed by Image J software (NIH).

Biochemical analysis

The samples were crushed and incubated in 100 μL of 1 M HCl solution at room temperature overnight, followed by neutralization via the addition of 5 M NaOH. The total protein and calcium contents of each sample were measured by using BCA protein assay kit and calcium quantification kit according to manufacturer's instructions, and the calcium contents were then normalized to total protein.

Histological analysis

Cells were fixed with 4% paraformaldehyde solution for 1 h at room temperature, and then the hydrogels were dehydrated in series of ethanol, cleared in series of xylene, and embedded in paraffin. The samples were sectioned to 8 μm thickness by Microm HM325 (Thermo, U.S.A.), and then rehydrated and stained for target of interests. For von kossa and alizarin red staining, the staining was performed according to manufacturer's instructions. For immunohistochemistry staining, the sections were incubated with collagen type I and osteocalcin primary antibodies at 4°C overnight with

gentle rocking, and then treated with vectorstain ABC kit and the DAB substrate kit according to manufacturer's protocol. The images were acquired by Ti-2 microscopy (Nikon, Japan), and analyzed by Image J software (NIH).

Simulation

The simulation was conducted by Monte Carlo method based on the classical motor-clutch model. It was adopted to determine/update the status (open or closed) of clutches. Specifically, the disassociation probability P of an engaged clutch during time interval Δt (5ms in this work) was described as

$$P = 1 - e^{-k_{off}\Delta t}. \quad (1)$$

Similarly, the rebinding probability of a broken clutch was expressed as $1 - e^{-k_{on}^{j}\Delta t}$ and the actin polymerization initiation probability is $1 - e^{-k_p\Delta t}$.

The implemented numeric scheme includes the following steps.

(1) Seed stiffen points and initialize a cell in a 2D plane.

(2) Determine whether new actin bundle polymerization happens, if yes, assign n_c clutches and n_m motors.

(3) Determine the substrate stiffness $k_s(r)$ at the leading edge.

(4) Calculate membrane resistance f_{mem} with cell periphery geometry.

(5) At each polymerization site

(i) Determine clutches status using Monte Carlo method with k_{off} and k_{on}^{j}.

(ii) Calculate $x_{c,i}^{j}$, x_s^{j} and $F_{c,i}^{j}$, F_{clutch}^{j}.

(iii) Calculate myosin motor force F_{myo}^{j} from Eq. (3).

(iv) Calculate retrograde flow rate V_f^j from Eq. (4).

(v) Calculate spreading rate V_s^j from Eq. (5).

(vi) Update the molecule density d_{int}^j.

(6) Advance leading edge position and return to step (2).

All the parameters adopted in this study are summarized in Table S1. Simulations were conducted for at least 300000 steps to ensure that the steady state has been reached.

Animal models

12-week-old male Sprague Dawley (SD) rats were randomly divided into 5 groups (Sham, GHG, GHG-PEGDA, GHG-NP50, GHG-AcNP50, n=3). A 5 mm diameter defect was created using a trephine with normal saline irrigation during processing, and the section of bone was removed to expose the dura mater. The hydrogels (5mm in diameter and 1 mm in thickness) encapsulated with 5×10^5 rat MSCs (rMSCs) were transplanted to the defects, then the soft tissues were closed. The sham group received the same surgery treatment without transplantation of hydrogels. All SD rats were sacrificed after 8 weeks, and the samples were harvested for the following μCT and histological analysis. All the animal experiments were conducted in accordance with the regional Ethics Committee guidelines, and all animal procedures were approved by the Animal Care and Use Committee of The Chinese University of Hong Kong.

Statistical analysis

All data are presented as mean ± standard deviation. Statistical analysis was performed by using one-way ANOVA and Tukey's honest significant difference (HSD) post hoc test of the means.

Supplementary simulation notes

It is conceivable that the presence of nanoparticles (i.e., AcNP30 and AcNP50) can increase the stiffness of hydrogel locally, promote the formation of stable cell-ECM adhesion and eventually enhance cell spreading. Specifically, it was assumed that, starting from a circular initial configuration, a cell begins to spread by extending/pushing (via actin polymerization) its membrane along all directions. An engaged clutch will disassociate from the substrate at a rate of k_{off} which increases exponentially with the force f_c acting on it, i.e., $k_{off} = k_0 e^{f_c/F_b}$. Here k_0 is the breaking rate of clutches under zero force and F_b represents a characteristic force (~ a few pN). On the other hand, a broken clutch can re-engage with the substrate with a rebinding rate k_{on}.

Interestingly, a recent study has demonstrated that a stiffer substrate will induce higher intracellular contraction which could then trigger conformational change of force-sensitive proteins (such as talin [5]) and ultimately lead to recruitment of adhesion molecules (i.e., integrin). In this study, such force-induced reinforcement of adhesion is phenomenologically described as $k_{on} = k_{on}^0 d_{int}$ where k_{on}^0 is a constant binding rate and d_{int} represents the normalized concentration (by a baseline value d_{int0}) of adhesion molecules [6], a quantity that is force dependent, refers to SI for details. In our experiment, the stiffness distribution of the fabricated AcNP30 or AcNP50 embedded

hydrogel has been examined via AFM scanning (Figure 2E, F). Interestingly, it was found that the measured local stiffening effect (near a nanoparticle at location r_c) can be well fitted by

$$k_s(r) = (k_s^{max} - k_s^0)e^{-\frac{|r - r_c|}{0.5}} + k_s^0 \quad (1)$$

where r is the position vector while k_s^{max} and k_s^0 stand for the maximum and basal stiffness, respectively.

Now, if we focus on the *j*-th intracellular actin bundle, the total clutch force acting on it can be expressed as

$$F_{clutch}^{\ j} = \sum_{i=1}^{N_{eng}^{\ j}} F_{c,i}^{\ j} = \sum_{i=1}^{N_{eng}^{\ j}} k_c(x_{c,i}^{\ j} - x_s^j) \quad (2)$$

where $N_{eng}^{\ j}$ is the number of clutches formed on the actin bundle, x_s^j and $x_{c,i}^{\ j}$ represent the displacement of the substrate and the i-th clutch, respectively (refer to "Conversion between the effective stiffness and elastic modulus of the substrate" part), and k_c corresponds to the stiffness of the clutch. In addition, the cell membrane will also exert a force $F_{mem}^{\ j}$ (refer to "Membrane resistance" part) on this polymerizing bundle to resist its advancement. These forces must be balanced by active myosin contraction ($F_{mot}^{\ j}$), trying to pull the bundle towards the cell center, that is

$$F_{mot}^{\ j} = F_{clutch}^{\ j} - F_{mem}^{\ j}. \quad (3)$$

Furthermore, assuming n_m myosin motors are acting on this bundle, then the moving speed of the bundle (often referred to as the retrograde flow speed) is expected to follow the Hill's law as

$$V_f^j = V_u\left(1 - \frac{F_{mot}^{\ j}}{n_m F_m}\right) \tag{4}$$

where V_u is the maximum retrograde speed and F_m represents the stall force for a single myosin motor. Under such circumstance, the spreading velocity (V_s^j) of the cell along this actin bundle is

$$V_s^j = V_p - V_f^j \tag{5}$$

where V_p is a constant polymerization velocity. Once V_s^j is known, the spreading distance can then be determined by simple forward Euler integration. As the spreading process progresses, V_f^j will increase gradually and eventually reach the level of V_p, leading to a steady-state shape of the cell.

Conversion between the effective stiffness and elastic modulus of the substrate

In our model, the deformability of the substrate is characterized by its stiffness k_s. On the other hand, in our AFM scanning test, distribution of the Young's modulus E of the material was obtained. Conversion between these two quantities can be made via the Green's function method as

$$k_s \approx \frac{2}{3}\pi R E \tag{6}$$

where R is the radius of the area covered by a single clutch. Since the diameter of an integrin is ~10 nm and the spacing between integrins within a focal adhesion must be less than ~58nm, *R* is estimated to be $17nm$ (i.e., the middle value) here.

From force equilibrium, the load transmitted to the substrate is the same as that acting on the actin bundle, that is

$$F_{sub}^{\ j} = F_{clutch}^{\ j}. \tag{7}$$

The resulting substrate deformation x_s^j can be determined by

$$F_{sub}^{\ j} = k_s x_s^j \tag{8}$$

or equivalently (from Eqs. (2), (S2) and (S3))

$$x_s^j = \frac{k_c \sum_{i=1}^{N_{eng}^{\ j}} x_{c,i}^j}{k_s + N_{eng}^{\ j} k_c} \tag{9}$$

Implementation of the reinforcement mechanism

Recent findings have demonstrated that different adhesion molecules, activated by large adhesion force, can assemble to form stronger focal adhesions on stiff substrate. To describe such force-dependent reinforcement of adhesion, the density of adhesion molecules $d_{int}^{\ j}$ (available to actin bundle j) was assumed to increase/decrease by a fixed amount Δd after a complete load and fail cycle from t_1^j to t_2^j once the time averaged force of all engaged clutches, defined as

$$F_{avg}^{\ j} = \sum_{t=t_1^j}^{t=t_2^j} w^j(t) f_{avg}^{\ j}(t) \tag{10}$$

surpasses/falls below a threshold value F_{cr}. Here $f_{avg}^{\ j}(t) = \frac{F_{clutch}^{\ j}(t)}{N_{eng}^{\ j}(t)}$ is the average force of engaged clutches (note that $F_{clutch}^{\ j}(t)$ is the total clutch force transmitted by $N_{eng}^{\ j}(t)$ engaged clutches at time t) and $w^j(t) = \frac{\Delta t}{t_2^j - t_1^j}$. It must be pointed out that $d_{int}^{\ j}$ was not allowed to drop below the initial density d_{int0} since no obvious adhesion growth will occur under this low level of concentration. Finally, we must emphasize that the approach adopted in this study is just one of many possible phenomenological

descriptions of how reinforcement of adhesion takes place.

Membrane resistance

The plasma membrane was assumed to have initial tension γ_0, area A_0 and area elastic modulus K_A. That is, as cell area A increases, the membrane tension γ grows as $\gamma = \gamma_0 + K_A \frac{A - A_0}{A_0}$. The membrane resistance acing on the polymerizing actin bundle therefore takes the form

$$F_{mem}^{j} = \gamma(C_1^j + C_2^j)\Delta A^j \tag{11}$$

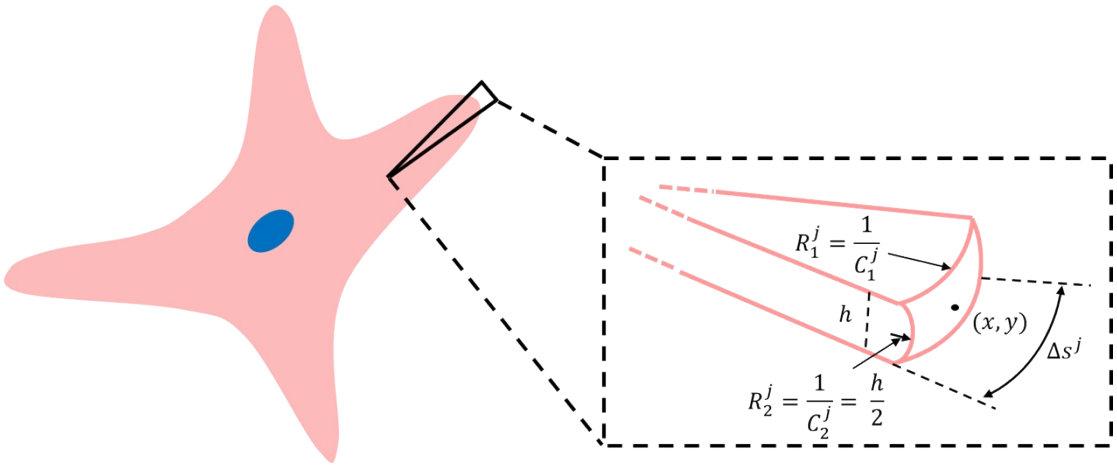

where C_1^j and C_2^j represent the principal curvatures of the deformed membrane. Specifically, if the rim of the spreading cell is assumed to have a uniform thickness h~$200nm$ then we have $C_1^j = \frac{x'y'' - x''y'}{(x'^2 + y'^2)^{\frac{3}{2}}}$ and $C_2^j = 2/h$ with x', y', x'' and y'' being the first and second derivatives of coordinates of leading edges. $\Delta A^j = h\Delta s^j$ is the effective local membrane area at protrusion position with arc length Δs^j (Figure S1).

Figure S1 Schematic diagram of a slice of cell membrane with arc length Δs^j and height h. Single actin bundle protrudes along (x, y) direction at middle height. The principal

radii of curvature of the deformed rim are denoted as R_1^j and R_2^j, respectively.

Influence of the number of actin bundles

In this study, 180 actin bundles (evenly distributed in all directions) were assumed to polymerize and push the cell membrane simultaneously. To test the influence of the number of actin bundles, simulations with double actin bundles but half polymerization velocity (to ensure the total polymerization energy is fixed) were also conducted. As shown in Figure S2, the actin bundle number does not affect the results in any significant manner.

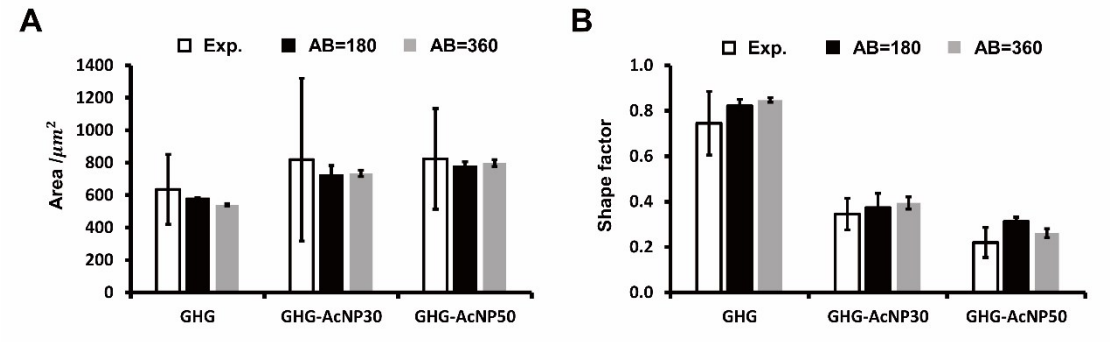

Figure S2 Results of the spreading area (**A**) and shape factor (**B**) of cells in different stiffness environments. Exp: experimental data; AB: number of actin bundles adopted in the simulation. Data are shown as mean ± standard deviation (n=5).

All the parameters adopted in this study are summarized in Table S1. Simulations were conducted for at least 300000 steps to ensure that the steady state has been reached.

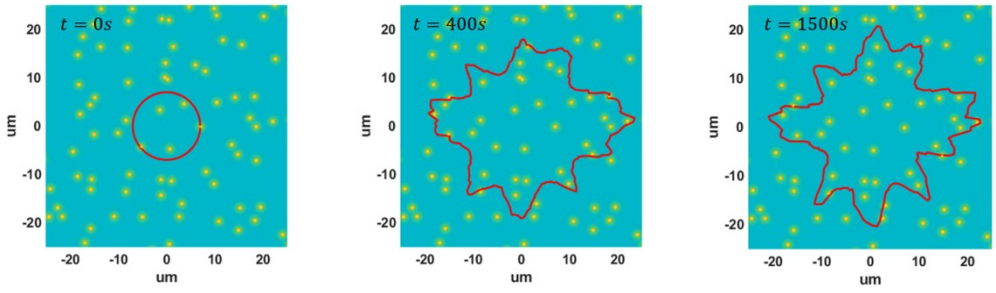

Figure S3 show the snapshots of the cell morphology obtained from our simulations.

Figure S3 Snapshots of the simulated cell morphology under a stiffen point density of $0.03\mu m^{-2}$.

Table S1. Parameters adopted in spreading model

	parameters	values
substrate	k_s^0	0.1068 pN/nm
		2.9908 pN/nm
	k_s^{max}	1.068 pN/nm
		0.2136 pN/nm
clutch	ρ	0.03 μm^{-2}
	n_c	300
	k_c	5 pN/nm
	k_{on}^0	0.15 s^{-1}
	d_{int0}	2500μm^{-2}
	Δd	100
	F_{cr}	2 pN
motor	k_0	0.1 s^{-1}
	F_b	2 pN
	n_m	100
	F_m	2 pN
actin	V_u	200 nm/s
	k_p	1 s^{-1}
	V_p	200 nm/s
	r_o	7 μm
membrane	h	200 nm
	γ_o	0.01 pN/nm
	K_A	0.04 pN/nm

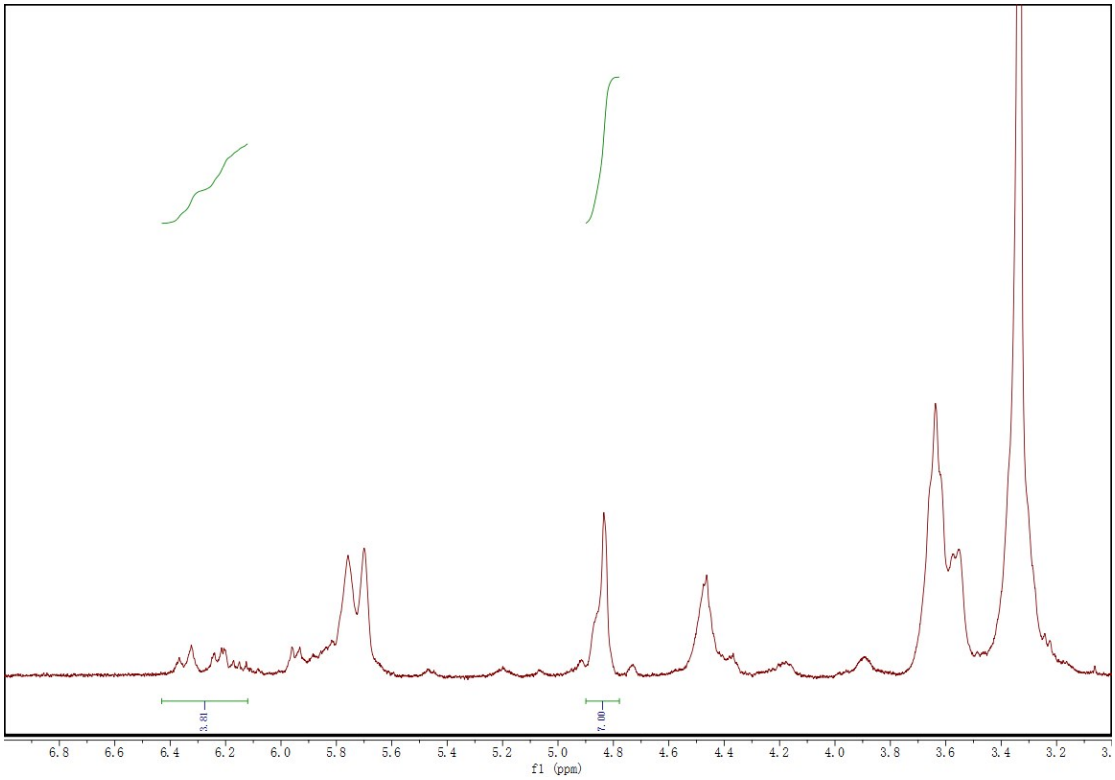

Figure S4 NMR spectrum of Ac-β-CD (S. D.=1.27).

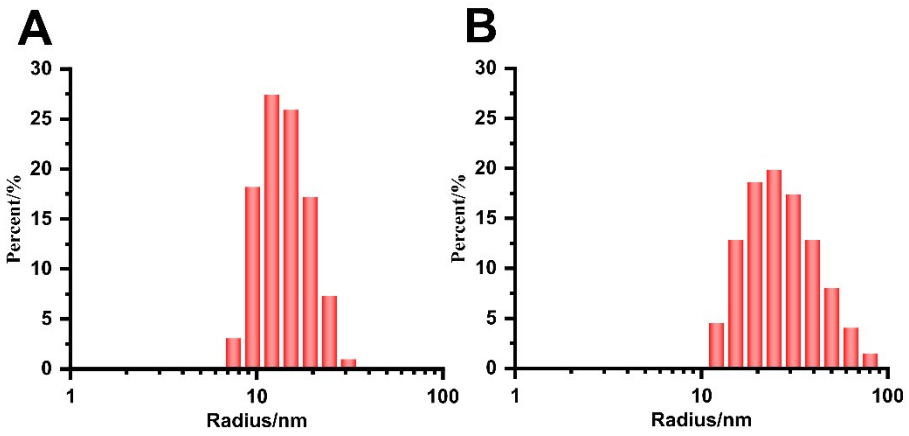

Figure S5 DLS measurement of (A) AcNP30, (B) AcNP50.

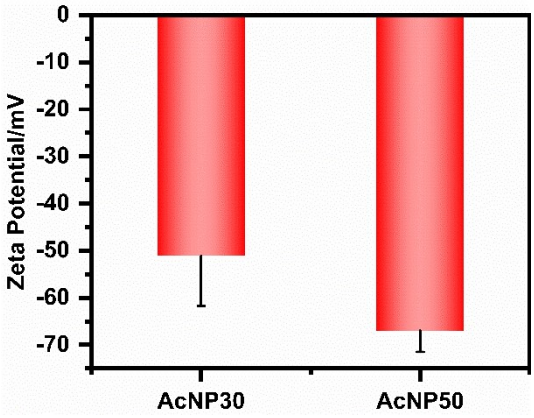

Figure S6 Zeta potential values of AcNP30 and AcNP50

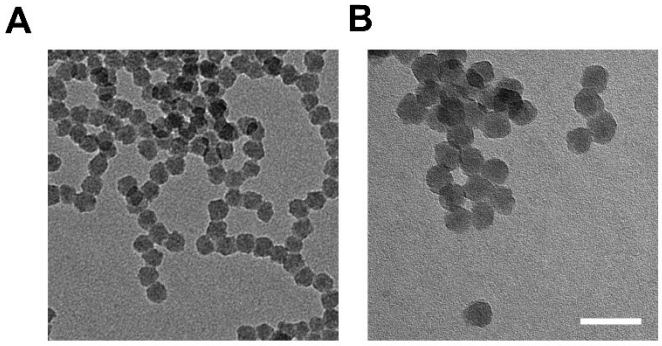

Figure S7 Representative TEM image of (A) AcNP30, (B) AcNP50. Scale bar: 50 nm.

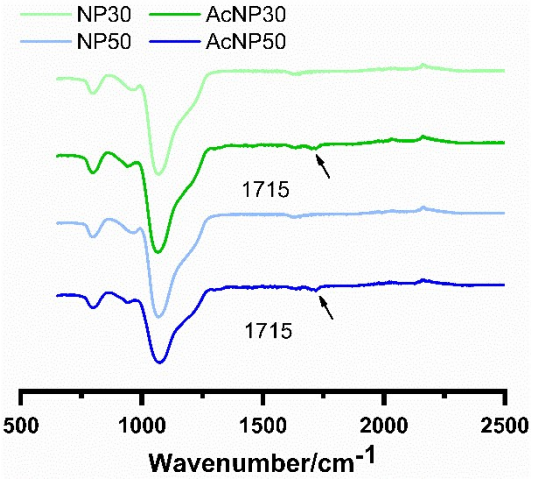

FigureS8 FT-IR spectra of NP30, AcNP30, NP50, and AcNP50.

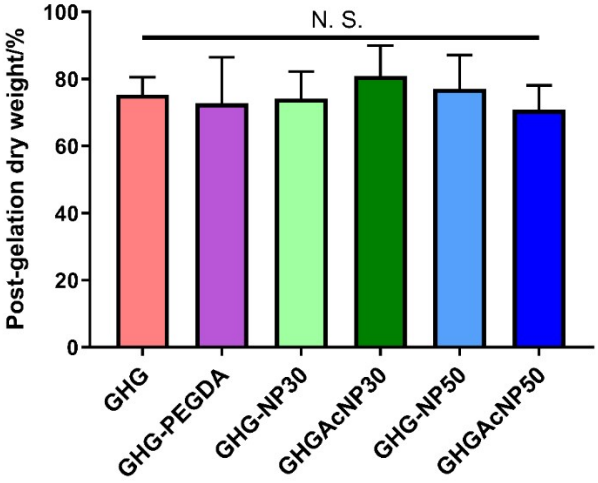

Fig. S9 Post-gelation analysis of the GHG, GHG-NP30, GHG-AcNP30, GHG-NP50 and GHG-AcNP50 hydrogels

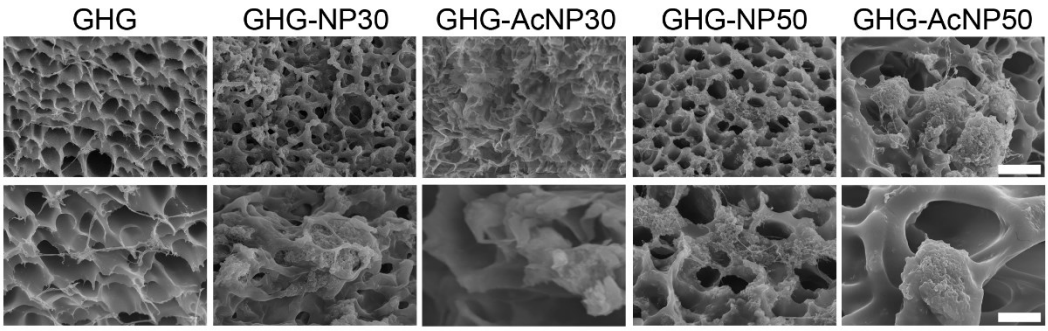

Figure S10 Representative cross-sectional interior structure of GHG, GHG-NP30, GHG-AcNP30, GHG-NP50 and GHG-AcNP50 hydrogels. Images on the top: scale bar=20 μm. Images on the bottom; scale bar=5 μm.

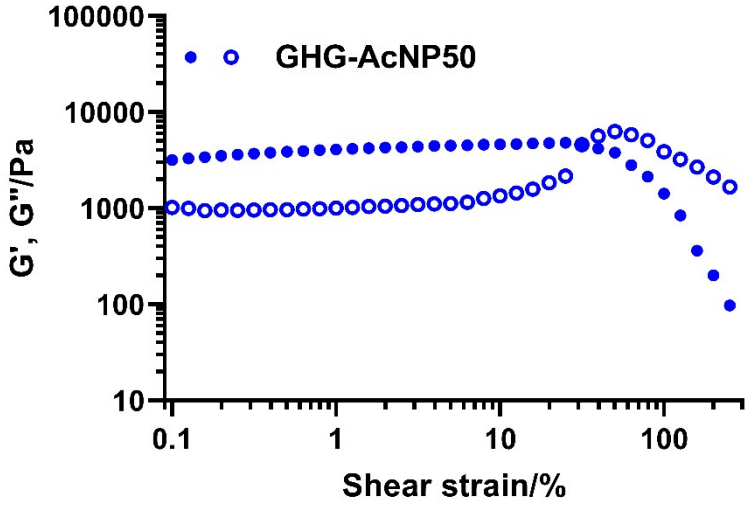

Fig. S11 The oscillatory strain sweep of the GHG-AcNP50 hydrogel

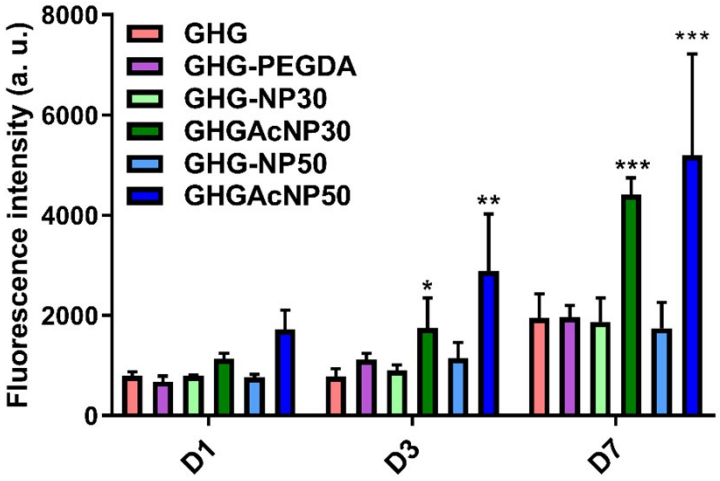

Fig. S12 The proliferation rates of the encapsulated stem cells in the GHG, GHG-NP30, GHG-AcNP30, GHG-NP50 and GHG-AcNP50 hydrogels

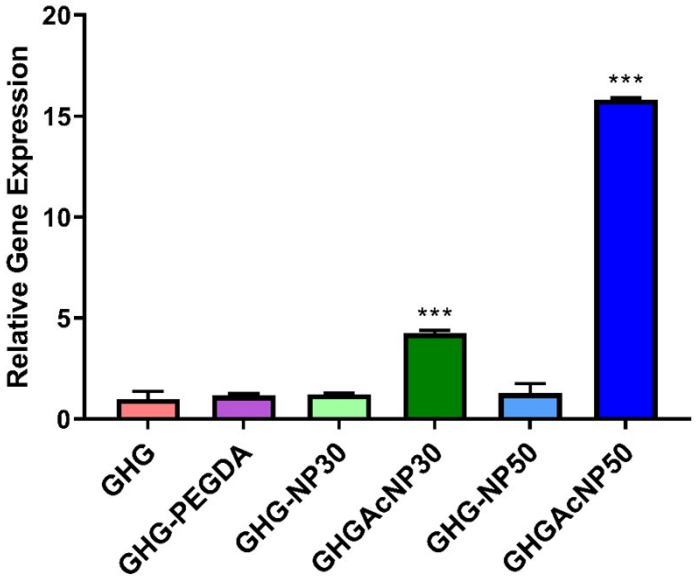

Fig. S13 Quantitative gene expression levels of the MAPK as determined by qPCR in the stem cells encapsulated in GHG, GHG-PEGDA, GHG-NP30, GHG-AcNP30, GHG-NP50 and GHG-AcNP50 hydrogels after 7 days in osteogenic culture.

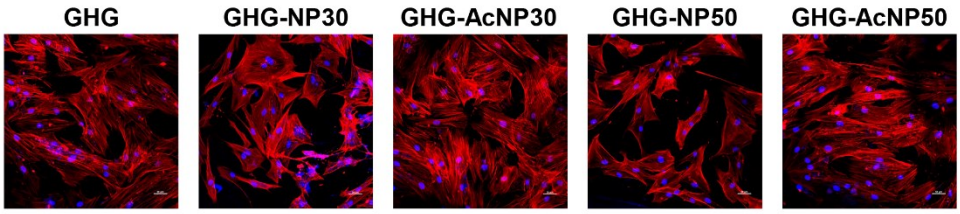

Fig. S14 Representative confocal laser scanning microscopy (CLSM) images of

hMSCs spreading on 2D hydrogel substrates.

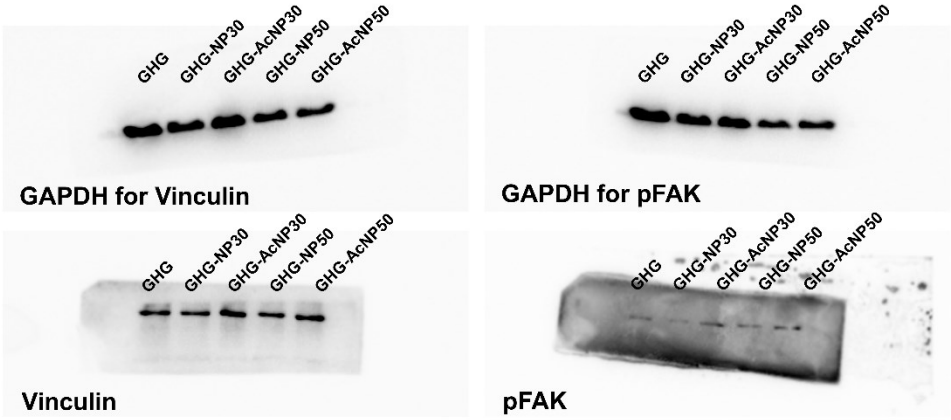

Fig. S15 Unprocessed images from the western blot analysis of vinculin and pFAK in hMSC-seeded hydrogels after 7 days of osteogenic culture.

Table S2. The sequences of the primers and probes used for qPCR are listed. The sequences of the primers and probes of the osteocalcin and Runx2 are proprietary (Thermo) and not disclosed.

Gene	Forward primer	Reverse primer	Probe
GAPDH	AGGGCTGCTTTTA ACTCTGGTAAA	GAATTTGCCATGG GTGGAAT	CCTCAACTACATG GTTTAC
COL I	AGGACAAGAGGC ATGTCTGGTT	GGACATCAGGCG CAGGAA	TTCCAGTTCGAGT ATGGC
ALP	CGGAACTCCTGA CCCTTGAC	TGTTCAGCTCGTA CTGCATGTC	TCGAAGAGACCC AATAGGT

Reference

1. Q. Feng, K. Wei, S. Lin, Z. Xu, Y. Sun, P. Shi, G. Li and L. Bian, *Biomaterials*, 2016, **101**, 217-228.
2. K. D. Hartlen, A. P. T. Athanasopoulos and V. Kitaev, *Langmuir*, 2008, **24**, 1714-1720.
3. D. M. Gao, Z. P. Zhang, M. H. Wu, C. G. Xie, G. J. Guan and D. P. Wang, *Journal of the American Chemical Society*, 2007, **129**, 7859-7866.